ELSEVIER

Biochimica et Biophysica Acta 1458 (2000) 6–27

BIOCHIMICA ET BIOPHYSICA ACTA
BBA

www.elsevier.com/locate/bba

Review

The mechanism of the proton transfer: an outline

Lev I. Krishtalik

A.N. Frumkin Institute of Electrochemistry, Russian Academy of Sciences, Leninskii prosp. 31, 117071, Moscow, Russia

Received 1 November 1999; accepted 1 December 1999

Abstract

A brief summary of the principal notions of the quantum–mechanical theory of the charge transfer reactions has been presented. In the framework of this theory, the mechanism of the proton transfer consists in the classical medium reorganization that equalizes the proton energy levels in the initial and final states, and a consequent proton transfer via a quantum–mechanical underbarrier transition. On the basis of this mechanism, factors influencing the proton transfer probability, and hence kinetic isotope effect, have been discussed; among them are the optimum tunneling distance, the involvement of the excited vibrational states, etc. Semi-classical and quantum–mechanical treatments of the Swain–Schaad relations have been compared. Some applications to enzymatic proton-transfer reactions have been described.

Keywords: Adiabatic process; Nonadiabatic process; Activation energy; Tunneling probability; Kinetic isotope effect

1. Introduction

Proton transfer is a ubiquitous component of the vast amount of various chemical and biochemical reactions. Therefore, the mechanism of this process presents a problem of primary importance. The first model of the elementary act of proton transfer was proposed by Horiuti and Polanyi [1]. In this model, the activation energy of the process was considered to be caused by the necessity to stretch the hydrogen covalent bond in proton donor to a distance at which formation of a bond with the proton acceptor becomes possible (Fig. 1A). The further development of this model proceeded by introduction of quantum–mechanical corrections. First, account was taken for the energies of zero-point vibrations, different for different hydrogen isotopes (Fig. 1B); in more sophisticated schemes involving multidimensional energy surfaces, the zero-point energies of transition state were also accounted for. Second, the proton (deuteron) tunneling at the top of the barrier was included (Fig. 1C). This approach, which we will name the bond-stretching model, was employed and developed in many works (for review see, e.g. [2–4]).

The bond-stretching model has two important drawbacks. First, it does not take into account the dynamic role of the polar medium: the proton transfer means a substantial charge density redistribution, and hence is inevitably coupled with the medium reorganization. Second, quantum–mechanical effects were included in the model as some ad hoc corrections while the problem demands for a consistent quantum–mechanical treatment just from the beginning. These two principally important points were laid in the basis of the approach proposed by Dogonadze et al. [5,6]. The theory developed results in the following general scheme of the process (Fig. 2): the medium reorganization equalizes the proton levels in the initial and final states, and hence makes the proton transfer possible, preferentially by a quantum–

0005-2728/00/$ – see front matter
PII: S0005-2728(00)00057-8

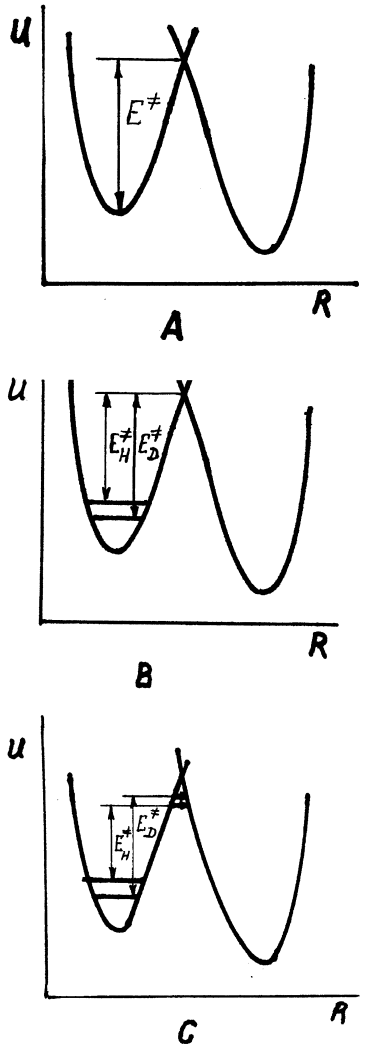

Fig. 1. Potential energy curves for proton transfer in the bond-stretching model. ***R***, proton coordinate; $E^{\neq}$ activation energy, subscripts H and D refer to proton and deuteron, correspondingly. (A) Original scheme by Horiuti and Polanyi [1]. (B) The scheme accounting for the difference in zero energies of two isotopes. (C) The scheme accounting for the tunneling at the top of the barrier (shown by arrows); the heavier isotope tunnels through the lower and narrower barrier.

mechanical underbarrier transition (a more detailed discussion of the mechanism will be given below). This mechanism is similar to that of the electron transfer process. The medium reorganization–proton tunneling model (or DKL model) was further developed in many works, mainly by Dogonadze–Kuznetsov group (see, e.g. [7–9]).

The bond-stretching and DKL models lead to similar general dependencies (e.g. of activation energy on the reaction free energy ΔG) because these dependencies are of a very general phenomenological nature [10]. However, one can find some effects where the two model result in not only quantitatively, but also qualitatively different predictions, and hence find some experimental criteria allowing a choice to be made between the alternative models. We have carried out such an experimental study on the example of an electrochemical proton transfer, viz. the rate-determining discharge of proton donors

$$AH^{n+} + M(e^{-}) = A^{(n-1)+} + MH$$

(here M means metal and e means electron). The effects of the electrode potential, of the metal nature (M–H bond energy), of different proton donors, and of the solvent on the hydrogen evolution reaction kinetic parameters and on kinetic isotope effect as well as the characteristics of the barrierless discharge (process with the activation energy equal to the reaction free energy, without any additional barrier) were studied. In all cases, it was shown that the activation energy and the pre-exponential factor are determined by physically different barriers; this agrees with the medium reorganization–proton tunneling model and contradicts the bond-stretching model. These data are summarized in [10,11].

Last decade, the great interest in the medium reorganization–proton tunneling model arises. The physical fundamentals of the model were not disputed, rather a further development of these ideas was given. The progress is connected, first of all, with the microscopic treatment of the medium reorganization (in earlier works, it was considered mainly in the framework of continuum electrostatics, with an account of quantum character of some polarization modes, and of possibility of the polarization spatial correlation). Further, various theoretical methods have been applied to the analysis of the problem giving, in general, a rather good agreement. A more detailed quantum–chemical calculations have been performed for several concrete systems. As typical examples, studies by Borgis and Hynes can be mentioned (see, e.g. [12] and a great many of the recent papers cited there), as well as those by Warshel and Chu [13], Cukier [14], Antoniou and Schwartz [15] and others.

The size of this short review does not allow to give a more or less full account of the vast literature on

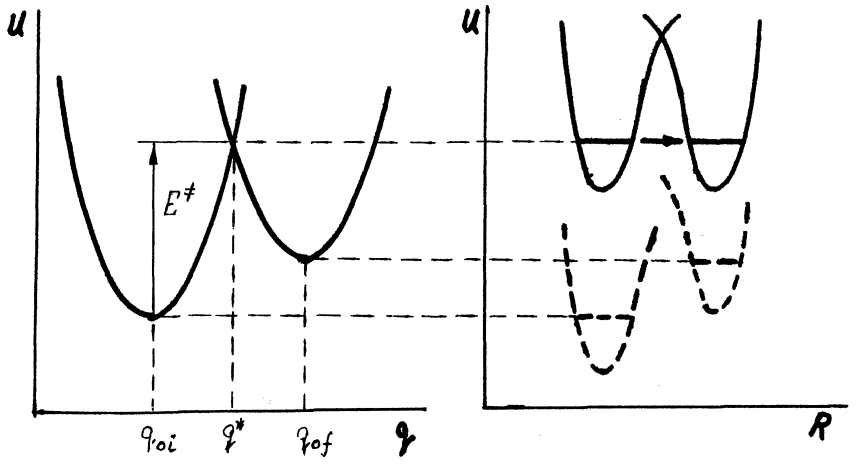

Fig. 2. Potential energy curves (cross-section of the potential energy surfaces) for the medium reorganization–proton tunneling model (DKL model). Left panel: the energy dependence on the medium coordinate q; $q_{0i,f}$ equilibrium medium coordinates in the initial and final states, q^* coordinate of the barrier top (crossing point), $E^{\neq}$ activation energy. The right panel: potential curves for proton at different constant medium coordinates, the dashed curves correspond to equilibrium states, initial and final ($q_{0i,f}$), the solid curves to transition state q^*. Only in transition state, the ground levels of proton in its initial and final potential wells become equal, and the tunneling becomes possible (shown by arrow).

the problem and to describe in detail the history of each question. The reader especially interested in the theory can be referred, besides the reviews and papers quoted above, to detailed monographs [16–18]. In this review, our task will be to outline the main features of the proton transfer mechanism and to elucidate qualitatively their physical basis. We will also apply this analysis to explanation of some experimental data.

2. General theoretical relationships

2.1. Quantum and classical degrees of freedom

As it was described above, in the DKL model proton, like electron, tunnels from one reactant to another after equalizing the energy levels created by the polar medium fluctuations (Fig. 2). It should be stressed here that it is not an ad hoc assumption, but a result of a rigorous theoretical analysis based on the concept of quantum and classical degrees of freedom [19]. Let us explain this concept.

With any barrier, there always exists a possibility of two different types of transition: overbarrier and underbarrier ones, and therefore one should compare the probabilities of these ways. The probability of the underbarrier transition (tunneling) by itself depends on the form of the barrier and on the energy (E) of the particle which is to tunnel. The energy dependence is very strong, roughly exponential (exp $E/\Delta E$). Here ΔE means some energy characteristic for the given barrier shape (by the order of magnitude, it is the difference of two neighboring discrete energy levels), it can be different in different parts of the barrier. On the other hand, one should account for the probability to be at the energy level E, i.e. to multiply the 'pure' tunneling probability by the Boltzmann factor $\exp(-E/kT)$. So, the total contribution of the level E is proportional to $\exp(E/\Delta E - E/kT)$.

There are two typical limiting cases. When $\Delta E \gg kT$, the probability is virtually $\exp(-E/kT)$, and the most probable process involves the lowest energy level $E=0$. This is a typical quantum behavior: the predominant process is the tunneling from the ground state. The second case corresponds to $\Delta E \ll kT$. Here the most favorable situation is for the highest possible level E, i.e. at the top of the barrier. Such a system behaves classically, i.e. an overbarrier transition dominates. Besides these limiting cases, the relationship $\Delta E \sim kT$ is possible; here the most favorable pathway is the thermal excitation to some intermediate level(s) with a subsequent tunneling somewhere in the middle of the barrier.

Electron is localized in a potential well formed by

some hyperboloid-like surface. The typical differences of the electron energy levels are much more than kT (absorption of the visible light or, mostly, UV quanta), and hence electron behaves in a quantum–mechanical manner.

The covalently bound proton presents an oscillator having in the ground state an approximately harmonic character (the characteristic energy ΔE is of order of $\hbar\omega$, ω is the vibration frequency). The typical vibration quanta for X–H covalent bond are of order of 3000 cm^{-1}, while $kT = 200$ cm^{-1} at room temperature. That is why we have to expect the quantum–mechanical behavior in reaction of proton transfer accompanied by disruption and formation of its covalent bonds (for more details, see below).

It is clear that the quantum–mechanical or classical behavior is not an inherent property of the system under any conditions. The system behaving classically at high temperature may become a quantum–mechanical one at very low temperature. For instance, this can explain the transition from the Arrhenius dependence of the reaction rate at room temperature to its temperature independence at low temperatures. Sometimes one can meet a statement that the process governed by tunneling shall always be temperature-independent, while the presence of some temperature dependence (at least, Arrhenius dependence) contradicts the tunneling. Indeed, the underbarrier transition probability proper does not depend on the temperature. However, tunneling becomes possible only in the case the energy levels in initial and final states are equal (only then a transition will not violate the energy conservation law). To equalize these levels, that, generally, are not equal from the beginning, some reorganization of the medium (interacting electrostatically with electron, proton, etc.) is necessary. This reorganization proceeds via thermal fluctuation, and the probability to achieve the necessary medium configuration is determined by an Arrhenius-like expression. Only in the case when medium behaves also quantum–mechanically, i.e. the temperature is low enough as compared to medium's vibration quanta, the total probability becomes temperature-independent. In the intermediate region, where medium's $\Delta E \sim kT$, a non-Arrhenius dependence takes place.

A more graphic demonstration of the relationships between quantum and classical modes can be presented in the following way. The underbarrier transition probability is proportional to the resonance integral $\int \psi_i V_{if} \psi_f dv$, where ψ's are wave functions in the initial (i) and final (f) states and V_{if} is the potential of their interaction. It is clear that the probability is the higher the stronger is the overlap of the wave functions, i.e. the higher is the probability for the particle in some element of volume to belong as well to the initial as to the final states.

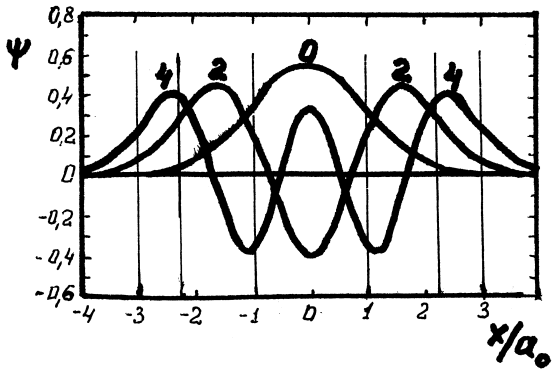

Fig. 3. Normalized wave functions (ψ) of a harmonic oscillator. Quantum numbers of the levels shown at ψ's maxima. Vertical lines mark the vibration's amplitude of a classic oscillator with the given energy.

The normalized wave function for a harmonic oscillator at some n-th level is (see, e.g. [20])

$$\psi_n = \frac{1}{\sqrt{a_n}}\left(\frac{1}{2^n n!\sqrt{\pi}}\right)^{1/2} H_n(s)\exp(-1/2)s^2). \quad (1)$$

Here a_n is the amplitude of classical vibrations at the n-th level [$a_n = a_0(2n+1)^{1/2}$], H_n is the n-th Hermite polynomial, $s = x/a_n$ is the reduced coordinate, x being the deviation from the equilibrium position. For the wave function at the ground level we have

$$\psi_0 = \frac{1}{\sqrt{a_0}\sqrt[4]{\pi}}\exp(-(1/2)(x/a_0)^2). \quad (1a)$$

Fig. 3 shows, as an example, the wave functions for $n = 0$, 2 and 4. We see that out of the classically accessible region (marked by a vertical lines) these wave functions decay with a similar speed. So, the classical amplitude in the ground state can be considered as a characteristic length determining decay of any wave function in the classically forbidden region.

Let us consider now the particle transition between two harmonic oscillators (Fig. 4 depicts their poten-

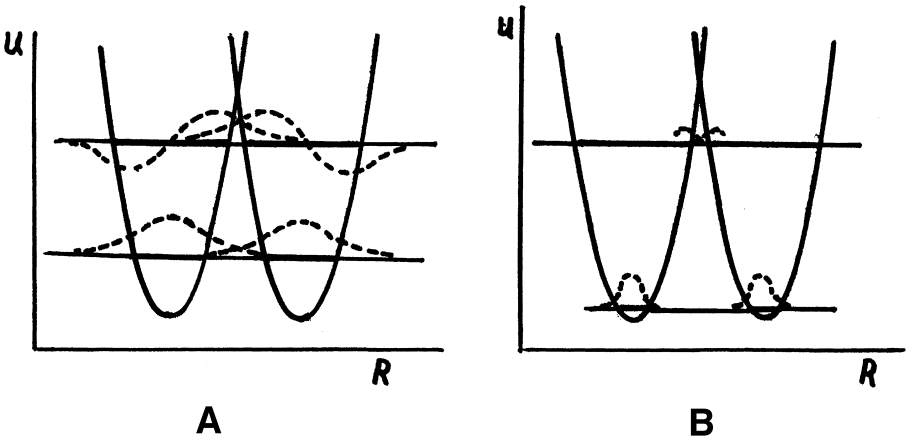

Fig. 4. Scheme of potential energy curves for two harmonic oscillators in the state where the particle transfer (along ***R*** coordinate) becomes possible (the levels are equalized due to the medium fluctuations: see, e.g. Fig. 2). The corresponding wave functions are presented in arbitrary units (dashed curves). (A) An oscillator with large $\hbar\omega$; the wave function overlap at ground level is substantial; also shown is the first excited vibrational level, much higher in energy. (B) The same potential curves, but with small $\hbar\omega$; the wave functions overlap at ground level is negligible; also shown is one of excited levels with a large quantum number, the wave functions are depicted conditionally, their overlap becomes tangible.

tial energy, two vibrational levels, and, in some arbitrary units, the wave functions corresponding to these levels). When the potential curves are steep and/or the oscillators reduced mass is small (both are typical of hydrogen covalent bonds), the zero-point energy (1/2 $\hbar\omega$) is large; correspondingly, the amplitude a_0 is large too, and the wave functions decay slowly (Fig. 4A). Therefore, the wave functions overlap is substantial already for the ground level, and the transition probability at this level is high enough to predominate over the transitions at excited levels (the overlap there is better, but the Boltzmann factor is low). Even with the same potential energy curves, but at a high oscillators reduced mass (Fig. 4B), 1/2 $\hbar\omega$ is small, so is the amplitude a_0, and the overlap is poor. In this case, the only realistic pathway is to excite the oscillator to very high levels, close to the barrier top, at which the transition probability is not negligibly low. Hence, when we speak on the quantum–behavior condition $\Delta E \gg kT$ (for harmonic oscillator, ΔE is practically $\hbar\omega$), we do not mean the difficulty to achieve some excited level (the Boltzmann factor for any level E is the same both for quantum and classical oscillators), but the larger delocalization of a quantum particle giving it the possibility to tunnel from the ground state. That is the reason why the underbarrier transition is preferential for the proton transfer.

2.2. Non-adiabatic and adiabatic transitions

In the preceding considerations, we have used potential curves (more strictly, free energy surfaces) corresponding to the initial and final states separately. These energy curves, unaffected by the reactants' interaction, are called 'diabatic curves'. However, interaction of the reactants influences the form of potential curves and the position of the corresponding energy levels. This is shown schematically, for the case of electron transfer, on Fig. 5. When the system is close to one of the energy minima, the states of the reactants are strongly dissimilar, the interaction between them is weak, and they do not form a unified state. Nearer to the barrier top, the energy of two reactants becomes similar, they can interact effectively, and they can form a unified state. More exactly, from two initially existing states (i and f) two new states appear, one which is lower than intersection point of the diabatic curves by the interaction energy V_{if}, and the other lying by the same value higher. These curves (free energy surfaces) are called adiabatic ones (U_+ and U_-, Fig. 5, left panel). Two adiabatic curves correspond to two different electronic states, and, instead of one energy level in each potential well (dashed horizontal lines in the right panel of Fig. 5), two levels appear (solid lines, Fig. 5, right).

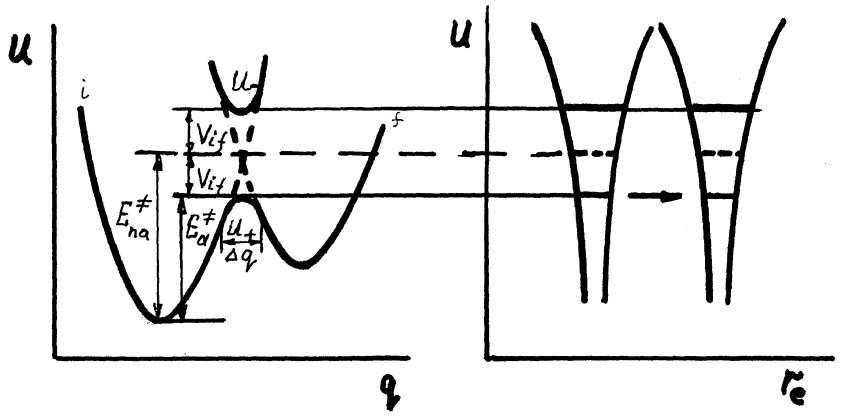

Fig. 5. Scheme of adiabatic electron transfer. Diabatic and adiabatic potential energy curves for classical subsystem (left panel). Crossing of diabatic curves (not affected by two partners' interaction) is shown by dashed lines. Interaction results in splitting of curves by $2V_{if}$, forming lower (U_+) and higher (U_-) adiabatic curves. Different activation energies for non-adiabatic and adiabatic transition are shown. The width of the region of substantial reactants interaction is marked as Δq. Right panel: potential energy curves for electron at initial (left) and final (right) positions. Dashed horizontal line, electron energy levels without reactants' interaction; solid lines, split electronic levels. The quantum subsystem (electron) undergoes the tunneling when the quantum level equalize, at the top of adiabatic U_+ barrier (the right panel of the figure).

When the system moves slowly from left to right along the polarization (classical) coordinate q (the left panel of Fig. 5), it is first in the initial diabatic curve (i), then it passes to the lower adiabatic curve U_+, and then goes over to the final curve (f); at the top of the adiabatic curve, electron goes under the barrier along the quantum coordinate r (the right panel of Fig. 5) remaining in the lower adiabatic state.

Such a pattern, however, can be realized only in the case of a slow enough movement along the classical coordinate. Indeed, the electron (and/or proton) transition from one potential well to the other (rearrangement of its wave function) takes some time τ_{if}. The transition can take place only in vicinity of the barrier top along the q coordinate: according to the Franck–Condon principle, the fast quantum–mechanical transfer proceeds at constant coordinates of all constituents of a slow classical subsystem, the energy of the quantum particle being constant (due to very different characteristic times of the classical and quantum motions, the quantum particle cannot borrow energy from the virtually immobile classical subsystem). On the other hand, the coordinate q is changing continuously, and the classical subsystem remains near the barrier top only for some restricted time τ_c. If this time is much longer than τ_{if}, the quantum particle can exchange many times between the reactants, the interaction leading to splitting of the energy levels can develop in a full extent, and hence adiabatic curves can form. In this case, at the top of the adiabatic q-barrier, the particle goes over from the initial position to the final one with the probability equal to 1.

In the opposite case, when $\tau_c \ll \tau_{if}$, the interaction between initial and final states does not have enough time to develop, the system remains in the diabatic state, and the barrier height is determined by intersection of the diabatic curves. In the course of its thermal fluctuations, the classical subsystem will pass the crossing point many times before the particle jumped to its final position. Therefore, at the top of the classical barrier, the transfer probability is much less than unity and is close, by order of magnitude, to the ratio τ_c/τ_{if}.

Let us estimate this ratio. The time τ_{if} is inversely proportional to V_{if} (the stronger the interaction, the more rapid is the transition). From dimensionality considerations, as the proportionality factor we can assume the Planck constant: $\tau_{if} \sim h/V_{if}$. On the other hand, $\tau_c = \Delta q/v^*$, where Δq is the width of the transition region (which lies in vicinity of the barrier top q^*, see Fig. 5, left), and v^* is the velocity of the system motion in this transition region. From the Franck–Condon principle, the transition proceeds at constant q and the system energy; the latter means

that the difference in energies of initial and final diabatic states, i.e. $|dU_i/dq - dU_f/dq|_{q^*}\ \Delta q$ should be compensated for by the interaction energy V_{if}. From the equality of these two quantities, the width Δq can be found. Substituting it into expression for τ_c, we can finally estimate the ratio τ_c/τ_{if}, so called adiabaticity parameter (Landau–Zener parameter γ):

$$\gamma = V_{if}^2/h\mathrm{v}* \left|\frac{dU_i}{dq} - \frac{dU_f}{dq}\right|_{q^*}. \quad (2)$$

The total transition probability P accounting for a many times passage of the system around the intersection point (at given energy, the classical oscillator moves back and forth along its diabatic curve) is

$$P = (1-e^{-2\pi\gamma})/\left(1-\frac{e^{-2\pi\gamma}}{2}\right). \quad (3)$$

At $2\pi\gamma \gg 1$, $P=1$ (adiabatic process), at $2\pi\gamma \ll 1$, $P=4\pi\gamma \ll 1$ (non-adiabatic process). A large adiabaticity parameter can be a result of different factors: strong interaction V_{if}, low velocity v*, and low slope of the initial and final diabatic curves ($dU_{i,f}/dq$; notice, that these two curves have the slopes of opposite sign, and therefore both corresponding terms in Eq. 2 are positive).

The medium can be described as some set of harmonic oscillators, or one oscillator with an effective frequency ω_{eff}. Then, for the transition probability per unit time we can write

$$W = \frac{\omega_{eff}}{2\pi}\kappa \exp\left(-\frac{\Delta G^{\neq}}{kT}\right). \quad (4)$$

Here $\omega_{eff}/2\pi$ gives the number of the system's oscillations towards the barrier top, $\exp(-\Delta G^{\neq}/kT)$ determines the fraction of these oscillations having the energy enough to reach the barrier top, and the transmission coefficient κ gives the probability of transition to the final state for a system which has reached the barrier (κ is essentially the same as Landau–Zener probability P; this designation is more usual in chemical kinetics).

Let us estimate κ using Eqs. 2 and 3. For a harmonic oscillator,

$$U = \frac{1}{2}\hbar\,(q-q_0)^2 \quad (5)$$

where q_0 is the equilibrium coordinate. Hence $|dU/dq| = \hbar\omega\,(q-q^0)$, the corresponding difference of derivatives is $\hbar\omega(q_{0f}-q_{0i}) = (2E_s\hbar\omega)^{1/2}$, the subscripts i and f mark the equilibrium coordinates of initial and final states, and E_s is the medium reorganization energy

$$E_s = \frac{1}{2}\hbar\,(q_{0f}-q_{0i})^2. \quad (6)$$

Exactly at the crossing point of two diabatic curves the total oscillators energy equals to its potential energy (kinetic energy is zero), and in vicinity of this point the system possesses kinetic energy of order of the average thermal energy $mv^2/2 = kT$. This equality, the expression for oscillators frequency $\omega = (f/m)^{1/2}$ and Eq. 5 give us the value of $\mathrm{v}* = (2\pi kT\omega/\hbar)^{1/2}$ (the coefficient $\pi^{1/2}$ appears due to averaging of velocities in some energies interval around kT). Substituting in Eq. 2 expressions for derivatives and velocity, we obtain the final result for transmission coefficient

$$\kappa = \frac{2\pi V_{if}^2}{\hbar\omega_{eff}}\left(\frac{\pi}{kTE_s}\right)^{1/2}. \quad (7)$$

The other useful form of Eqs. 4 and 7 is

$$W = \frac{V_{if}^2}{\hbar}\left(\frac{\pi}{kTE_s}\right)^{1/2}\exp\left(-\frac{\Delta G^{\neq}}{kT}\right). \quad (8)$$

For the non-adiabatic reaction, the activation energy $\Delta G^{\neq}$ is determined by intersection of two diabatic curves and is expressed through reorganization energy E_s and the free energy of the elementary act G_0 by the usual quadratic expression of the Marcusian type

$$G^{\neq} = \frac{(E_s + \Delta G_0)^2}{4E_s}. \quad (9)$$

For adiabatic reaction, the activation barrier is determined not simply by crossing of two diabatic curves, but is lower by the value of the interaction energy V_{if} (see Fig. 5, left panel).

Let us consider briefly the influence of the medium vibration frequency on the reaction rate. As is seen from Eqs. 4 and 7, in non-adiabatic processes ω_{eff} enters the rate equation both in numerator and denominator, and hence cancels out (this is presented explicitly in Eq. 8). The physical reason of that is clear: an increasing ω_{eff} means more crossings the barrier in a time unit, but simultaneously a larger

velocity of this crossing, and hence a decrease in τ_c and in transition probability at each crossing.

In adiabatic process, the medium frequency enters the rate equation explicitly. However, one remark seems to be expedient here. In the real medium, there is a lot of different vibrational modes of different frequencies. The effective value of Eqs. 4 and 7 should be obtained by averaging the squared frequencies of all modes weighted proportional to their contributions into activation energy. Because the squares are averaged, the dominant is the highest frequency present in a tangible proportion. Usually, it is the frequency close to the classical limit (note, that only classical subsystem moves over the barrier). This limit is $kT/\hbar$, hence for the totally adiabatic process we obtain the usual pre-exponential of the transition state theory kT/h. In the above considerations (as well as in the transition state theory), it was accepted that there does exist a thermal equilibrium distribution of all microconfigurations (corresponding, in particular, to various dipoles orientations). If the rate of the thermal equilibration is not high enough (high viscosity, conformational rigidness of the proteins structure), the characteristic relaxation time enters the pre-exponential of the rate equation of an adiabatic reaction (see, e.g. [21–25]).

3. Proton transfer

3.1. The principal regimes of proton transfer

Up to this point of our discussion, we have not specified what a quantum particle is considered, electron or proton, and they really have much common in their behavior. However, there exists a substantial difference between them: the characteristic time of electron movement is by approximately one order of magnitude shorter than that of proton. Therefore, we should consider not only adiabatic or non-adiabatic behavior of some quantum particle relative to movement of the classical subsystem (medium polarization), but also the problem if electron follows adiabatically proton movement or not.

When proton goes under the barrier from its initial to final well, at the proton coordinate $\boldsymbol{R}^*$ (the top of the barrier along $\boldsymbol{R}$) some rearrangement of the electronic cloud should proceed leading to disruption of A–H bond and formation of a new B–H bond. The time of this rearrangement should be compared with the time of proton residence in vicinity of $\boldsymbol{R}^*$. So, here appears a new adiabaticity parameter, described by the same Eq. 2, but with the other meaning of velocity v*. This velocity is no more the velocity of classical movement, but the absolute value of the imaginary velocity of proton inside the classically prohibited region under the barrier. Further, the derivatives of $U_{i,f}$ should be taken relative to proton coordinate. If the adiabaticity parameter, determined in such a way, $2\pi\gamma_{tunn} \ll 1$, then we have a totally non-adiabatic process, both electron and proton do not follow adiabatically the medium movement, and electron does not follow proton's motion (as a matter of fact, this case, with a low proton tunneling probability, was depicted in Fig. 2).

In this case, the interaction matrix element in Eqs. 7 and 8 is the electron–proton one, and it is determined as

$$V_{ep} = \int \psi_{pi} V_{if} \psi_{pf} dv \approx V_{if} \int \psi_{pi} \psi_{pf} dv = V_{if} \exp\left(-\frac{1}{2}\sigma\right) \quad (10)$$

where σ is the tunneling factor determined by the overlap of the vibrational wave functions of proton in A–H (i) and in B–H (f) corresponding to the coordinate q^* of the surrounding medium (the top of the barrier along q). Eqs. 7 and 8 take the form

$$\kappa = \frac{2\pi V_{if}^2 \exp(-\sigma)}{\hbar\omega_{eff}} \left(\frac{\pi}{kTE_s}\right)^{1/2} \quad (7a)$$

$$W = \frac{V_{if}^2}{\hbar} \left(\frac{\pi}{kTE_s}\right)^{1/2} \exp(-\sigma) \exp\left(-\frac{\Delta G^{\neq}}{kT}\right). \quad (8a)$$

For a totally non-adiabatic reaction, activation energy will be determined by Eq. 9.

At the opposite relationship, $2\pi\gamma_{tunn} > 1$, electron follows adiabatically proton motion during its under-barrier transition. However, proton transition can be, at the same time, non-adiabatic ($\kappa \ll 1$). In this case, proton behaves non-adiabatically relative the medium while electron follows proton adiabatically.

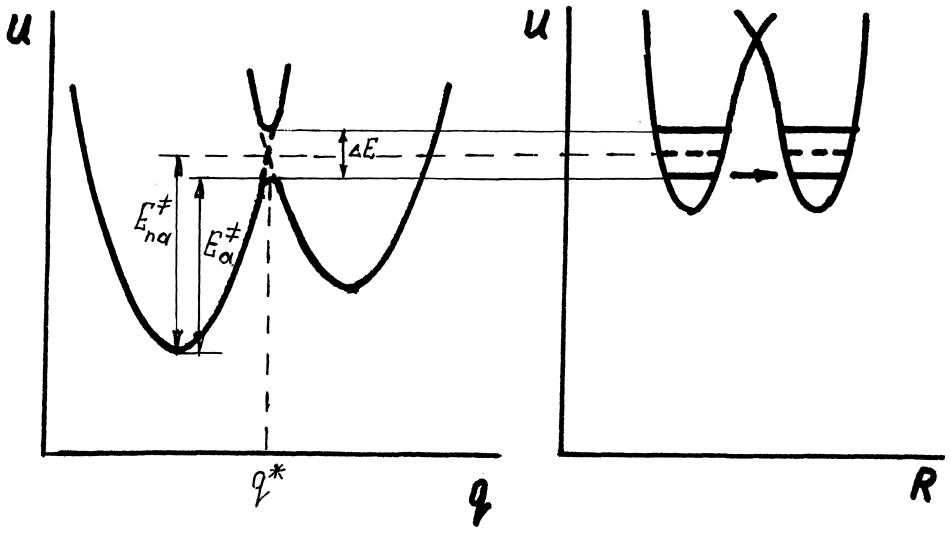

Fig. 6. Scheme of adiabatic proton transfer. The figure is similar to Fig. 5. Diabatic and adiabatic potential energy curves for classical subsystem (left panel). Right panel: potential energy curves for proton at initial (left) and final (right) positions. Reactants interaction splits proton vibrational level by ΔE.

This process can be called a partially adiabatic (or partially non-adiabatic) reaction [7].

For the partially adiabatic reaction, expressions similar to Eqs. 7 and 8 are valid, but with the following difference: the half of the vibrational levels splitting $\Delta E/2$ should be substituted for V_{if}. This splitting is connected with the tunneling factor through

$$\Delta E \approx \hbar\Omega_p \exp\left(-\frac{\sigma^{ad}}{2}\right) \quad (11)$$

where Ω_p is the frequency of the proton vibration, and σ^{ad} refers to the tunneling under the adiabatic barrier. Similar to adiabatic electron transfer, the activation barrier is lowered here by corresponding interaction energy, i.e. by $\Delta E/2$. However, for partially adiabatic process, the proton wave functions overlap is weak, and hence the splitting of vibrational levels ΔE is small. So, activation energy is practically close to that calculated by Eq. 9.

For the sake of simplicity, we have not accounted for the existence of several discrete vibrational levels in both initial and final state, for each combination of them its own κ should be introduced. The total reaction probability should be found as a sum of probabilities of all partial transfers.

In simple chemical reactions, it can be often assumed that electrons of the two transformed covalent bonds follow adiabatically the proton movement, i.e. a partially adiabatic process takes place. However, in some biological, especially bioenergetic processes, we meet the situation of a concerted proton and electron transfer, electron being transferred from a rather distant donor. In this case, a totally non-adiabatic transfer can be expected.

When all γ's are more than unity, the process proceeds totally adiabatic. For totally adiabatic process the transmission coefficient $\kappa = 1$. Large γ is caused by good overlap of all wave functions, including protonic ones. Therefore, in the totally adiabatic process splitting of the vibrational levels can be substantial, and this may result in a marked correction to activation energy (see Fig. 6).

3.2. Some typical cases of proton transfer

As we have seen, the probability of proton transfer (tunneling factor σ) depends strongly on the overlap of its vibrational wave functions. An important quantitative parameter of the oscillator's wave function is the vibration amplitude of a corresponding classical oscillator. For a typical A–H covalent bond with a stretching vibration frequency about 3000 cm^{-1} the zero-point vibration amplitude $a_0 = 0.1$ Å. This is the characteristic length determining, in the first approximation, the proton transfer mechanism.

Let us consider the case when the proton donor and acceptor are held at some large distance, so that the distance between two minima is of order of several angstroms. It is easy to conclude that in this case the tunneling probability at the ground level is negligibly small. For such a large distance, the donor–acceptor interaction is weak, and hence the splitting of vibrational levels is negligible, as is shown in Fig. 7. At large deviations from the equilibrium positions, the anharmonicity of the corresponding oscillators is substantial, and therefore the curves acquire the shape depicted in Fig. 7. The underbarrier transition becomes possible only near the top of the barrier, i.e. the system behaves virtually classically, both for proton and medium movements; electron follows them adiabatically. The activation energy consists of the barrier along the polarization coordinate q (not shown) and the barrier along the proton coordinate $\boldsymbol{R}$. The last one, due to the curves anharmonicity, is close, by order of magnitude, to the bond dissociation energy. So, we can expect here an activation energy of order of many tens of kilocalories; that means the proton transfer on large distances of several angstroms is improbable.

Let us go over to the proton transfer at the distance of the order of 1 Å or less. Here it is expedient to consider two types of systems, viz. with a weak or strong donor–acceptor interaction. To the first type belong the couples involving C–H acids and/or corresponding bases, metallic electrode in electrochemical proton discharge, systems with hydride anion transfer, etc. The second type of systems includes the proton donors and acceptors forming a well-expressed hydrogen bond.

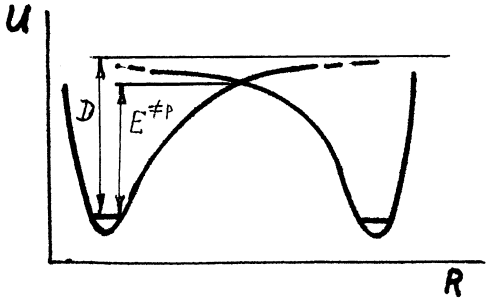

Fig. 7. The potential curves for proton transfer at the top of the medium barrier (q^*). The distance between reactants is very large, Morse-like character of potential curves is well pronounced, the reactants' interaction is weak, and hence the resonance splitting of energy levels is practically negligible. The activation energy component due to proton movement $E^{\neq p}$ is close, by order of magnitude, to the bond dissociation energy D.

In the weakly interacting systems, the equilibrium distance between donor and acceptor equals the sum of their van der Waals radii. At the neutral H radius $\sim$1.2 Å, typical acceptor atom radius $\sim$1.5 Å, and the covalent bond length $\sim$1.1 Å, the equilibrium distance between two minima is $\sim$1.6 Å. This is too large as compared to 0.1 Å, and hence the proton transfer in this position is strongly unfavorable. However, the tunneling probability increases drastically with the closer approach of reactants. As can be seen from Eqs. 1 and 1a, proton wave function decays exponentially with the distance squared. Therefore, the tunneling probability depends exponentially on the square of the tunneling distance

$$\exp(-\sigma) = \exp\left(-\frac{m}{\hbar}\frac{\Omega_i\Omega_f}{\Omega_i+\Omega_f}(\Delta\boldsymbol{R})^2\right). \tag{12}$$

Here m is the reduced mass (practically, mass of H atom), $\Omega_{i,f}$ proton frequencies in the initial and final states, $\Delta\boldsymbol{R}$ is the distance between two minima (tunneling distance). Decrease in the tunneling distance increases the tunneling probability.

On the other hand, the approach of the reactants cannot be an unrestricted one because repulsion between reactants hinders their mutual approach. The repulsion energy can be described by, e.g. Born–Mayer potential

$$U = B\mathrm{e}^{-\frac{\boldsymbol{R}}{\rho}} \tag{13}$$

where $\boldsymbol{R}$ is the distance between two heavy atoms ($\Delta\boldsymbol{R}$ plus length of two covalent bonds), B and σ are empirical constants. The total transfer probability is proportional to

$$\exp\left(-\frac{m}{\hbar}\frac{\Omega_i\Omega_f}{\Omega_i+\Omega_f}(\Delta\boldsymbol{R})^2\right)\exp\left(-\frac{B\exp\left(-\frac{\boldsymbol{R}}{\rho}\right)}{kT}\right). \tag{14}$$

The two opposite trends result in some optimal distance ensuring a maximum of expression (Eq. 14), i.e. the high enough tunneling probability and,

at the same time, not too large energy expenditure necessary to overcome the repulsion. The estimates for proton transfer between two C atoms carried out with realistic constants borrowed from independent experimental data have shown that the optimum tunneling distance is much shorter than the equilibrium one: about 0.4 Å instead of 1.5 Å [26]. The empirical parameters used in these calculations were, of course, only approximate ones. Furthermore, the formula for non-adiabatic tunneling of protons in a double well of two harmonic oscillators was employed, and hence the donor–acceptor interaction even at small inter-reactant distance was neglected. Therefore, the result of these calculations cannot be considered as a strict and quantitative one. Nevertheless, it shows unambiguously that, in a transition configuration, a very substantial approach of the reactants should take place, and gives the realistic order of its magnitude. It should be mentioned that the calculations employing, instead of harmonic, a Morse potential for C–H and O–H covalent bonds and substituting another Morse potential for C...O interaction have resulted in a quite similar value of the optimal tunneling distance, viz. 0.46 Å [9].

As is seen from Eq. 14, the optimum distance depends, generally speaking, on temperature, and this may cause some deviations from the Arrhenius equation.

The other type of systems present O–H and similar acids reacting with O, N and other bases. The donor–acceptor interaction is rather strong already under equilibrium conditions, and the hydrogen bond is forming. For typical O–H...O bond with O...O distance of 2.8–3.0 Å and the O–H bond length of 1 Å, the equilibrium inter-minima distance equals to 0.8–1.0 Å. This is also somewhat too large for an effective proton tunneling, and hence some approach of the reactants is necessary. In contrast to the previous case, the process is facilitated by two circumstances. First, the inter-reactant interaction makes the approach substantially easier than described by Eq. 13; the energy dependence on the distance is described here by a Morse-like equation with a much more gentle energy rise upon decrease in the O...O distance. Second, the energy curve along the proton coordinate deviates substantially from two intersecting parabolas of harmonic oscillators. Correspondingly, barrier along this coordinate is lower, and the tunneling probability is higher, and is not obeying Eq. 12. The form of the corresponding dependence can be determined, in principle, from quantum–chemical calculations. In particular, at not too short distances, it follows an exponential form $\exp(-a\Delta\boldsymbol{R})$ similar to this for the long-range electron transfer, but with much larger coefficient a (about 30–40 $Å^{-1}$ against ~ 1 $Å^{-1}$ for electron transfer [27]). As a result, proton transfer for the reactant of the first type is usually markedly slower than for those of the second.

With the inter-reactant distance decreasing, the barrier for proton tunneling becomes narrower, and this favors proton tunneling. Initially, at rather large distances, proton tunnels in the upper part of the barrier, and electron follows it adiabatically (partially adiabatic process). Upon further approach, the tunneling at the ground level becomes most favorable, the (imaginary) proton velocity rises, and the process becomes totally non-adiabatic. At a shorter distance, the barrier height (along $\boldsymbol{R}$ coordinate) decreases, the proton velocity decreases, and the process goes over to a partially adiabatic regime. A more closer approach can make the interaction so strong that the parameter $2\pi\gamma$ exceeds unity, and the process becomes totally adiabatic. But this adiabatic process differs from the case of very large distances: in the latter proton moves classically, but at very short distances, a fast tunneling of proton takes place. Further, at very short distances, the lowest vibrational level lies over the barrier top, and proton belongs to both molecules simultaneously (Fig. 8A). In a limit-

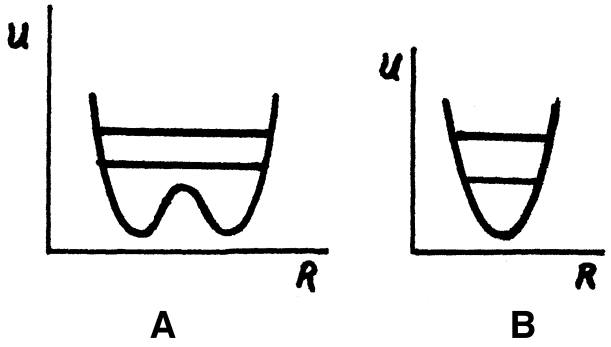

Fig. 8. Potential energy curves at very short distances between proton donor and acceptor. (A) The double-well potential curve with common vibrational levels. (B) Two wells have merged into a single one.

ing case, a one-minimum well is formed (Fig. 8B). An equilibrium structure, corresponding to situation depicted on Fig. 8, can be formed sometimes by extremely strong interacting molecules; this is a very short hydrogen bond (shorter than ~2.5 Å). For these systems, the question of proton transfer loses its sense.

It is understandable that variations in the reaction parameters can be very large depending on the effective potentials along O...O and H coordinates. This potential is affected both by the direct reacting atoms (e.g. OH and O) interaction and by the influence of groups bonded to O atoms; the latter can affect the O...O approach via, e.g. steric hindrances. In the latter case, reaction rate is substantially lower.

A specially interesting case presents the system with strong inter-reactant interactions (but weaker, than in couples with a very short hydrogen bond) and without any additional obstacles for the reactants movement. In such a system, the molecules can reach such a short distance that the single lowest vibrational level becomes common for both potential wells or even a one-minimum well, i.e. something like a very short hydrogen bond appears, but only as an non-equilibrium, transient configuration (Fig. 8). In that case, the proton tunneling becomes unnecessary, and the reaction rate will not depend on the proton movement, but will be determined by the rate of the molecules approach (the same will be for the case of a very fast, strongly adiabatic proton tunneling). Close to such behavior is, probably, proton transfer along the chain of highly mobile water molecules in some channels [28].

4. Kinetic isotope effect

Substantially quantum–mechanical character of the proton movement results, for many processes, in a very well expressed kinetic isotope effect (k.i.e.). Therefore, studies of k.i.e. become one of the most important tools for the proton transfer investigations, both experimental and theoretical. The presence of k.i.e. is considered as an evidence that proton transfer is involved in the rate-determining step (or, at least, in one of the steps affecting the reaction rate). On the other hand, absence of k.i.e. is widely accepted as a line of evidence for the rate-determining step not involving proton transfer. We will address this problem at the end of this section.

A vast literature exists on the topic, a review of many data can be found in [2–4]; the k.i.e. in enzymatic reactions was also reviewed many times, particularly detailed in [29–33]. Here, we will try to discuss some important features of the phenomenon from the point of view of the proton transfer theory described above.

4.1. K.i.e. at constant donor–acceptor distance

As we have discussed previously, the usual situation in the proton transfer mechanism is the donor and acceptor approaching to the distance favorable for proton tunneling, and, at the same time, not too close to result in an excessive repulsion energy. This optimal distance should be, generally speaking, different for the light and heavy isotopes. However, under definite conditions, the distance can remain the same for all isotopes. We will start our discussion with this case, the simplest from the theoretical point of view.

The situation is depicted in Fig. 9 (for the sake of clarity, we accepted here that pK of both donor and acceptor are the same; the effect of ΔpK will be discussed below). At the crossing point of the curves for classical subsystem, the levels of the quantum one equalize, and the proton (deuteron) tunneling become possible. Both for H and D, the levels are the same, the activation energy is the same, as determined by classical subsystem (see Fig. 9), and hence there is no effect of different zero-energy on the k.i.e. Only the tunneling probabilities are different, and hence the k.i.e. is determined only by this difference, i.e. by variation of pre-exponential factors (Eqs. 7a and 8a). This result is opposite to the conclusions of the bond-stretching model (in semi-classical approximation, Fig. 1B, the activation energies should be different; account for the tunneling at the top of the barrier, Fig. 1C, cannot change this conclusion). So, for the process at fixed distance, we have to expect, in the framework of the reorganization–tunneling model, a temperature-independent k.i.e. (the correction for non-equal difference of zero energies in initial and final states, which applies for non-equal pK of the donor and acceptor, will be considered later;

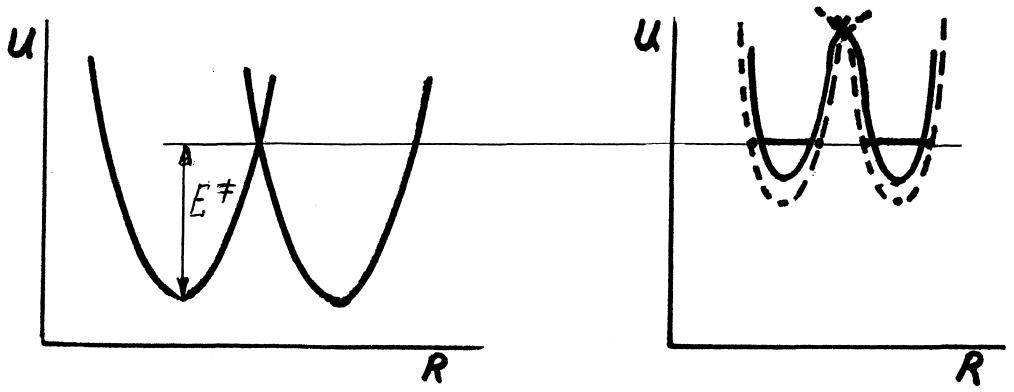

Fig. 9. Left panel: potential curves along the classical coordinate q; as pK of donor and acceptor are supposed to be the same, the reactions $\Delta G = 0$ (both minima at the same level). Right panel: potential curves along the proton coordinate: dashed for the light isotope and solid for the heavy one.

its value is usually small, on the verge of the experimental accuracy).

A constant tunneling distance may be expected in the case when the distance between donor and acceptor is determined not by necessity to optimize proton transfer, but by some other factor. One example of such a situation we can find in the enzymatic hydrolysis by serine proteases. For ester hydrolysis, the rate determining is deacylation step, more precisely, formation of a tetrahedral intermediate:

$$\begin{aligned}&\text{Asp-102–}CO_2^- + \text{His-57-Im} + H_2O + \begin{array}{c}R\\|\\C\text{–O–Ser-195}\\\|\\O\end{array} =\\ &\text{Asp-102–}CO_2^- + \text{His-57-Im}H^+ + \begin{array}{c}R\\|\\HOC\text{–O–Ser-195}\\|\\O^-\end{array}\end{aligned} \qquad (15)$$

The optimal disposition of heavy atoms is determined by the closest possible approach of O atom of attacking nucleophil (H_2O) to C of carbonyl group. The O–C distance should be the same for both light and heavy water, and the O–N distance (N is the proton-accepting atom of the His-57 imidazole ring) is as short as compatible with the geometry of mutual disposition of H_2O, C=O, and Im. So, the O–N distance is not optimized separately for H and D transfer, and remains the same for both isotopes. We have studied some hydrolytic reactions catalyzed by α-chymotrypsin [34,35] and β-trypsin [36]. A typical example is given in Fig. 10. In all cases, practically the same activation energy was found for reactions in H_2O and D_2O, i.e. k.i.e. was temperature-independent. In absence of the activation energy difference, k.i.e. can be determined only by the difference in pre-exponentials, i.e. by the difference in tunneling probability. To the best of my knowledge, this was the first demonstration of proton tunneling in an enzymatic reaction.

K.i.e. for serine proteases is not high, k_H/k_D about 3. This is, probably, due to rather favorable conditions for proton tunneling: donor, O–H, and acceptor, N, are connected with a hydrogen bond. In contrast, extremely large k.i.e., $k_H/k_D = 48$ was observed by Klinman and coworkers [37] in the lypoxigenase

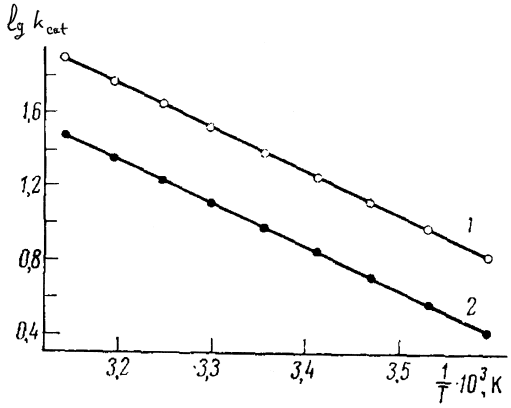

Fig. 10. Arrhenius dependence of the catalytic rate constant for hydrolysis of *N*-benzoyl-L-arginine ethyl ester catalyzed by β-trypsin [35]. 1, In H_2O; 2, in D_2O. Equal slopes of these curves mean equal activation energy for H and D transfer.

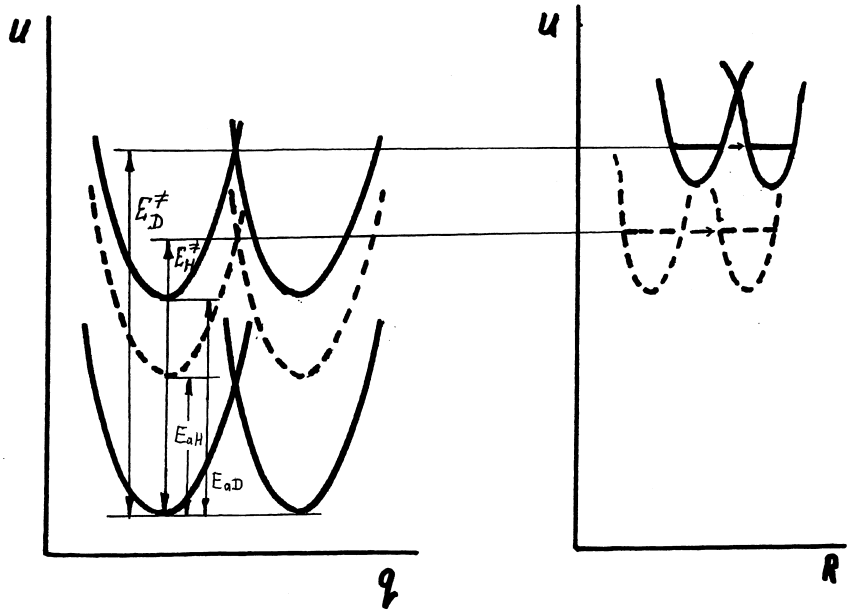

Fig. 11. Left panel: potential curves along the classical coordinate q. For the sake of clarity, pK values of donor and acceptor are supposed to be equal. The same is accepted for the repulsion energies between A–H and B (initial state) and A and B–H (final state). E_{aH}, E_{aD}, energies of approach of the H or D species to the optimal tunneling distance; $E_H^{\neq}$, $E_D^{\neq}$, effective activation energies of H and D transfer; $E_{H,D}^{\neq} = E_{aH,D} + E_i^{\neq}$, where $E_i^{\neq}$ is the activation energy of the proton (deuteron) transfer in the optimal configuration; as a good approximation, $E_i^{\neq}$ is the same for all isotopes (see Fig. 9). The lowest curves in the left panel relate to the reactant being at the van der Waals' distances, the upper ones to reactant at the distances optimal for tunneling, dashed for the light isotope and solid for the heavy one. Right panel: potential curves along the proton coordinate. Dashed for the light isotope and solid for the heavy one; the ground levels in initial and final states for each of the isotopes are equal. The shorter distance for deuteron tunneling is shown.

reaction. The details of enzyme structure and reaction mechanism are yet to be elucidated, but an important point is clear: proton (or H atom) is abstracted here from C–H bond, and hence one cannot suppose its hydrogen bonding to an acceptor. Therefore, in this reaction, one should expect proton tunneling under a rather high and wide barrier, resulting in a large k.i.e. Very weak temperature dependence observed suggests that, by some unknown reason, in this system the tunneling distances for proton and deuteron are similar.

4.2. K.i.e. at different tunneling distances

In the case when there are no special restrictions upon the mutual movement of the proton donor and acceptor, they will approach up to some optimal tunneling distance (see Section 3.2). This optimal distance will be different for light and heavy isotopes: tunneling of the latter is more difficult, and hence it is favorable, in this case, to spend more energy against repulsion forces, but decrease the tunneling distance. For instance, in the model discussed in [26], the optimal tunneling distance for H, D, and T were calculated to be equal to 0.393, 0.336 and 0.300 Å, respectively. In another model calculations [9], typical tunneling distances for H and D about 0.46 and 0.40 Å were obtained.

The energy diagram is depicted schematically in Fig. 11. The shorter optimal tunneling distance for deuterium transfer means a larger energy expenditure to arrive to this distance, and, hence, the higher effective activation energy as compared to protium transfer. Therefore, as a most common case, one should expect a substantial temperature dependence of k.i.e. It should be mentioned also that, as it was discussed in Section 3.2), the optimal tunneling distance is, in principle, temperature-dependent, and this may result in deviations from the linear Arrhenius plot, stronger for the heavier isotope.

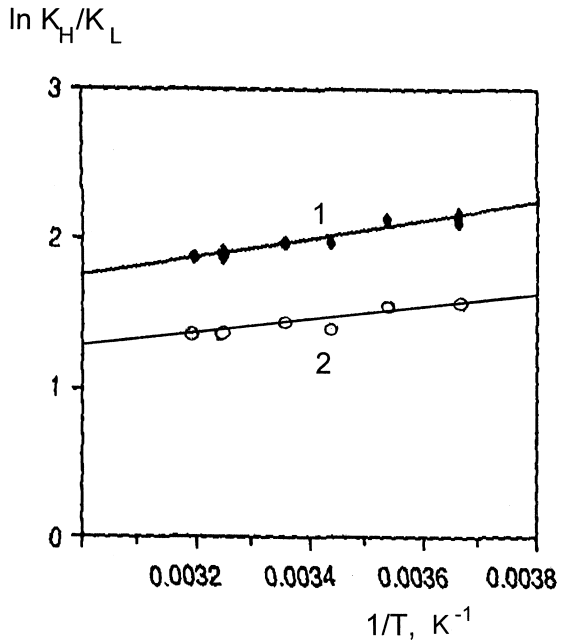

Fig. 12. Arrhenius plots for primary k.i.e. in oxidation of benzyl alcohol catalyzed by yeast alcohol dehydrogenase; curve 1 for k_H/k_T, curve 2 for k_H/k_D (reproduced after [39]). Substantial temperature dependence of k.i.e. points to a substantial difference in activation energies of transfer of three isotopes.

Klinman and coworkers have carried out an extensive investigation of H, D, and T isotope effects for several enzymatic reactions, and came to conclusion on a substantial role of tunneling in these processes (reviewed in [38,39]). As the reactions studied involved breaking of C–H bond, the observed effects were quite large. Except lipoxygenase reaction described above, all of them show a very well expressed temperature dependence of k.i.e. That could be expected because in all these reactions the heavy atom movement can influence the tunneling distance. As an example, the data on yeast alcohol dehydrogenase [40] can be shown (Fig. 12). In this reaction, proton abstraction from C–H bond to some base takes place.

4.3. Relationship between k.i.e. involving different isotopes

In many studies of k.i.e., based on the bond-stretching model supplemented by tunneling at the top of the barrier, the relationship between k_H, k_D, and k_T has been used as a criterion of tunneling [4,29–33,38,39]. From the point of view of semi-classical treatment, activation energy of reaction is $A-E_0$ where E_0 is the zero energy; for any isotope, $E_0 = E_{0H}/\sqrt{m}$, E_{0H} being the zero energy for protium, and m is the relative mass of the given isotope. From this considerations, the ratio of rates for two isotopes can be easily expressed as

$$k_i/k_k = \exp[E_{0H}(1/\sqrt{m_i}-1/\sqrt{m_k})]/RT$$

and hence

$$k_i/k_k = (k_m/k_n)^X \text{ where } X = (1/\sqrt{m_i}-1/\sqrt{m_k})/\,(1/\sqrt{m_m}-1/\sqrt{m_n}). \quad (16)$$

Most often studied ratios are

$$k_H/k_T = (k_D/k_T)^{3.26} \text{ and } k_H/k_T = (k_H/k_D)^{1.44} \text{ (Swain – Schaad relations).} \quad (16a)$$

Experimental values of X exceeding 3.26 (or, correspondingly, 1.44) are considered as evidence for a substantial tunneling contribution.

However, this conclusion is based entirely on semi-classical bond-stretching model (with tunneling corrections), but was never tested in comparison with predictions of the reorganization–tunneling mechanism. Remember that, in the latter model, the proton tunneling takes place almost in all cases (the only exception is when two proton vibrational ground levels merge together, see Fig. 8B). The corresponding relations in the framework of this mechanism will now be discussed.

According to Eq. 12, the tunneling probability can be presented in the form

$$\exp[-a_{0H} f(\boldsymbol{R})\sqrt{m_i}]$$

where $f(\boldsymbol{R})$ is a function of tunneling distance, a_{0H} is a constant related to protium, and the square root of the reduced mass of isotope i appears because frequencies are inversely proportional to $\sqrt{m}$. This expression is practically valid not only for harmonic oscillator, but, with another form of $f(\boldsymbol{R})$, for tunneling through other barriers too [15] (remember that Gamow equation for tunneling probability at any barrier form contains $\sqrt{m}$).

Under condition of constant tunneling distance $\boldsymbol{R}$, the ratios of rate constants are:

$$k_i/k_k = \exp[-a_{0H} f(\boldsymbol{R})(\sqrt{m_i}-\sqrt{m_k})]$$

and hence

$$k_i/k_k = (k_m/k_n)^Y \text{ where } Y = (\sqrt{m_i}-\sqrt{m_k})/(\sqrt{m_m}-\sqrt{m_n}) \quad (17)$$

and

$$k_H/k_T = (k_D/k_T)^{2.31} \text{ and } k_H/k_T = (k_H/k_D)^{1.76}. \quad (17a)$$

We see that exponents in Eqs. 16, 16a, 17 and 17a are different though of the same order of magnitude. Eqs. 17 and 17a are derived for conditions of a constant tunneling distance. As has been discussed before, the most frequent case is when the distance is different for all isotopes, being shorter for the heavier one. Therefore, in real systems, deviations from Eqs. 17 and 17a should be expected. The extent of these deviations depends on the relative influence of the reactants approach on the rates of all isotopes transfers (note that the effect is not simply change of $f(\boldsymbol{R})$, but also appearance of an additional contribution to activation energy: see, e.g. Eq. 14).

Let us consider effect due to variations of the optimal tunneling distance (and other similar effects too). With corrections (relative to H) p_T and p_D,

$$k_H/k_T = k_{0H}/k_{0T}p_T,\ k_D/k_T = k_{0D}p_D/k_{0T}p_T,\ k_H/k_D = k_{0H}/k_{0D}p_D$$

where k_{0i} are the constants at the distance of the optimal H tunneling, we obtain

$$k_H/k_T = (k_{0D}/k_{0T})^Y\ 1/p_T = (k_D/k_T)^Y\ (p_T)^{Y-1}/(p_D)^Y = (k_D/k_T)^Y(p_T/p_D)^Y/p_T \quad (18a)$$

$$k_H/k_T = (k_{0H}/k_{0D})^Y\ 1/p_T = (k_H/k_D)^Y(p_D)^Y/p_T = (k_H/k_D)^Y(p_D/p_T)^Y\ (p_T)^{Y-1}. \quad (18b)$$

Both factors p_T, $p_D > 1$, and $(p_T/p_D) > 1$ too: the heavier the isotope is, the stronger is the tunneling distance effect. Taking into account the numerical values of Y in Eqs. 18a and 18b (2.31 and 1.76, respectively), one can show that if the correction in Eq. 18a is larger than 1, the correction in Eq. 18b will be smaller. Correspondingly, the apparent exponential will be larger or smaller than calculated by Eq. 17a. Precisely this situation can be observed in the results of numerical calculations given below. We see that an account of the tunneling distance effect shifts the results of quantum–mechanical analysis towards the figures corresponding to semi-classical formulae, and, at more pronounced distance effect, they can exceed the latter. So, the system may have parameters close to the semi-classical Swain–Schaad relations, but this does not mean that the system behaves really semi-classically. The deviations from Eq. 16, in the reorganization–tunneling mechanism, do not mean larger or smaller extent of tunneling: tunneling is predominant in all cases.

The effect of the reactants approach was considered in [9,26]. Though the model calculations give reasonable order of magnitude for k.i.e., the calculated deviations from the Swain–Schaad relations are very sensitive to parameters used: e.g. for the parameters of repulsion potential employed in the text of [26] the values of Y were calculated to be 2.56 and 1.65, correspondingly, with other parameters of the same model the exponentials were 8.05 and 1.14 [26], for hydrogen-bonded reactants the values of 2.77 and 1.56 were obtained.

The isotopic rate constants ratio can be influenced by another effect: different involvement of vibrationally excited states, especially pronounced at large ΔG (see Section 4.4). I do not know any calculations where effect on the exponentials was analyzed with account of two factors simultaneously.

4.4. pK dependence of k.i.e.

In pK dependence of k.i.e., there are two contributions which will be consider separately. The first effect is illustrated by Fig. 13. The difference in pK can be ascribed to the different energies of the corresponding X−H bonds. This results in some difference in zero-point energies E_0 in the initial (i) and final (f) states, both for H and D (and hence, in corresponding difference of true pK values). As E_0 for H is $\sqrt{2}$ times larger than for D, $(E_{0f}-E_{0i})_D = (E_{0f}-E_{0i})_H/\sqrt{2}$. So, the equilibrium energy gap for protium differs from that for deuterium by $(E_{0f}-E_{0i})_H\ (1-1/\sqrt{2})$, and the change of activation energy equals fraction α of this value (α is the Brønsted coefficient determined by the ratio of the slopes of potential curves; under usual conditions, at $\lambda > |\Delta G|$, the value of α is around 0.50). When pK

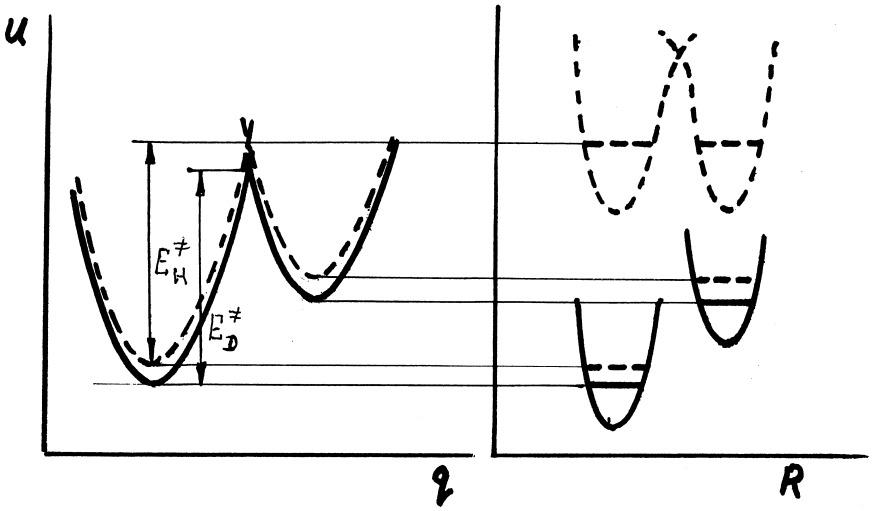

Fig. 13. Left panel: potential curves along the classical coordinate q. The minima of these curves correspond to the ground levels in the equilibrium initial and final states shown in the right panel. Right panel: potential curves along the proton coordinate; ground levels dashed for the light isotope and solid for the heavy one. Besides two equilibrium curves, those in transition state are shown. For the sake of clarity, the last curves are given only for the light isotope.

of donor is higher than of acceptor, $E_{0f} < E_{0i}$, the correction diminishes activation energy for H transfer as compared to D, at the opposite sign of ΔpK, the effect is also opposite.

Let us estimate the possible magnitude of this effect. According to an empirical rule, E_0 is proportional to the bond energy D [41]

$$E_0 = 0.042\ D \tag{19}$$

or, accepting that $\Delta pK = \Delta D/2.3\ RT$

$$\Delta E_0 = 0.058\ \Delta pK. \tag{19a}$$

At typical $\Delta pK \approx 6$ (e.g. difference of pK of side chains His and Ser), we obtain a correction to activation energy of only about 0.05 kcal, and a correction factor in primary isotope effect of order of 1.09 (these values increase up to about 0.1 kcal and 1.18, if an estimate for the effect of two bending vibrations will be added). This is smaller than the corresponding experimental errors.

The second effect, which plays a more important role, is the effect of participation of vibrationally excited levels. The corresponding energy diagrams are presented in Fig. 14. The minima of curves for classical subsystem (central panel) are shifted vertically according to the equilibrium energies of the ground and the first excited vibrational levels for H and D (right panel). Several transitions between vibrational levels are possible: $0 \rightarrow 0$, $0 \rightarrow 1$, $1 \rightarrow 0$ and $1 \rightarrow 1$. For the $0 \rightarrow 0$ transition, the activation energies for H and D are rather close (as it was discussed above, Fig. 13). However, due to smaller vibrational quanta for deuterium, the difference in positions of 'classical' (central) curves for H and D for excited state increases: $\hbar(\omega_H - \omega_D)$ instead of $\hbar(\omega_H - \omega_D)/2$ for ground level. Therefore, for some of transitions (in Fig. 14, it is $0 \rightarrow 1$ transition for deuterium), activation energy is albeit higher, but not too high as compared to $0 \rightarrow 0$ transition. At the same time, overlap of vibrational wave function for excited state is better (the barrier is lower and narrower) than in the ground state (Fig. 14, left panel). Therefore, contribution of the excited state is not negligible. This contribution is relatively larger for D than for H because for the latter, the excited level lies markedly higher.

Participation of excited vibrational states is possible, in principle, at any ΔpK, including $\Delta pK = 0$. However, this effect increases markedly with increase in $|\Delta pK|$. Indeed, for the situation depicted in Fig. 14 (an exergonic process, pK of donor is less than of acceptor), the lower is the energy of the product, the lower are the intersection points of potential curves D0 in the initial state and D0 and D1 in the final one (central panel). The closer is the intersection point to the curve's minimum, the smaller is α, i.e. the ratio

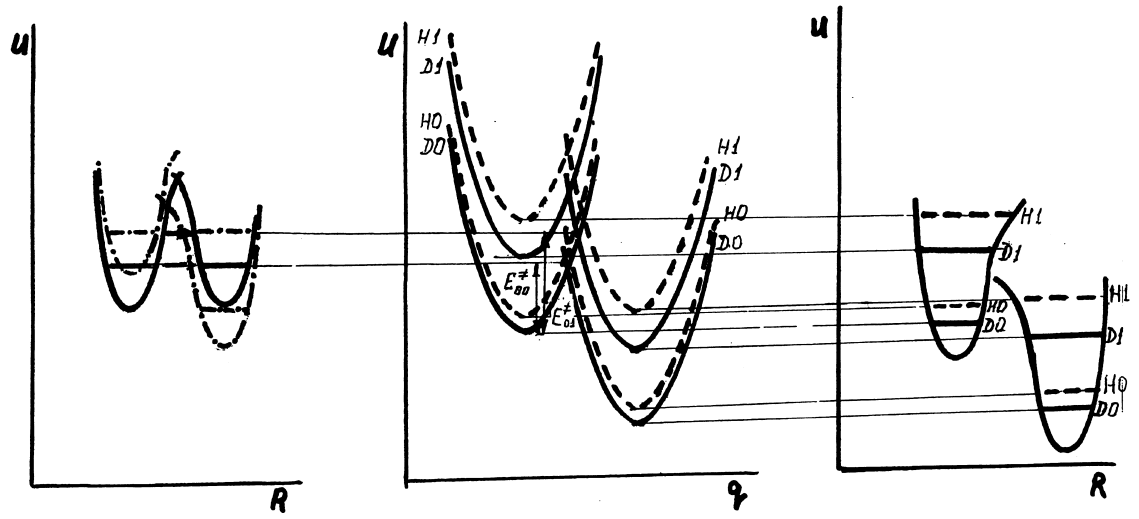

Fig. 14. Central panel: potential curves along the classical coordinate q. The minima of these curves correspond to the ground and first excited levels (marked D0, D1 and H0, H1, respectively) in the equilibrium initial and final states shown in the right panel. Activation energies for deuteron transfer from the initial ground level to final ground ($E^{\neq}_{00}$) and first excited ($E^{\neq}_{01}$) levels are shown. Right panel: potential curves along the proton coordinate in equilibrium state: ground and first excited levels dashed for the light isotope and solid for the heavy one. Left panel: potential curves along the proton coordinate in transition state; deuteron transitions from the ground to the ground and first excited levels are shown (initial state on the left, and final state on the right. Solid lines, 0–0 transition; dash-and-dotted lines, 0–1 transition).

of the slopes. This means that activation energy decreases for excited state with increasing ΔpK faster than for the ground state, and the relative contribution of the $0 \rightarrow 1$ transition increases. For H transfer, the effect of excited level is less pronounced than for D, and hence with increasing ΔpK transfer of D accelerates stronger than of H. So, increase in ΔpK decreases k.i.e. With the opposite sign of ΔpK, for endergonic process, the most important additional contribution originates from $1 \rightarrow 0$ transition. By similar considerations, in this case, k.i.e. also decreases with increasing absolute value of ΔpK. So, we see that participation of different excited vibrational levels explains well qualitatively (and, in model calculations, semi-quantitatively) the bell-shaped dependence of k.i.e. on ΔpK (with a maximum close to $\Delta pK = 0$) that was observed experimentally in several homologous series of acids (bases) [9]. Strong experimental arguments in favor of substantial involvement of excited levels were obtained recently [42] for electrochemical discharge of proton donors: in this case, much smaller bond energy of hydrogen adsorbed on metal results in smaller vibrational quanta what makes the excited states more easily accessible.

4.5. Secondary k.i.e.

When transfer of one of protons is coupled with a substantial change of position of another hydrogen atom (e.g. in the case of changing of hybridization of carbon orbitals), a secondary k.i.e. can be observed. The secondary hydrogen can move to its new location quantum–mechanically, i.e. by tunneling. Here, the tunneling distance is much shorter, and should proceed along the coordinate connected not with valence (stretching) vibration, but rather with bending vibrations (notice that the typical hydrogen bending frequencies are about 1500 cm^{-1}, i.e. substantially higher than kT). Secondary k.i.e. are, naturally, much lower than the primary ones. Experimentally, the ratios of isotopic rate constants for secondary hydrogens were found to be very sensitive to various factors [38,39]. The general approaches described above should be applicable for this problem too. However, a strict theory of secondary k.i.e. has yet to be developed.

4.6. Proton inventory method

For many enzymatic reactions, a question arises,

how many protons are transferred in the rate-determining step. A classical example of this problem is the mechanism of action of serine proteases: is it an one-proton reaction (as was presented in Eq. 15), or the second proton is transferred simultaneously from the other side of imidazole moiety to the nearby Asp (so-called 'charge-relay mechanism' [43])? The problem is often addressed by means of the proton inventory method (for review see, e.g. [4,44]). The method is based on the study of the dependence of the reaction rate on the atomic fraction of D in a mixed medium (usually, H_2O–D_2O mixtures). The treatment of the data employs the following formula (Gross–Butler equation) obtained by summing up the partial rates due to all isotopically different species:

$$k_n = k_0 \overset{m}{\Pi}(1-n+n\phi_i*)/\overset{m}{\Pi}(1-n+n\phi_i). \quad (20)$$

Here, the product involves all m reacting proton sites, k_n is the rate constant at the atomic fraction of D equal to n, k_0 is the same at $n=0$, ϕ_i and ϕ_i* are the fractionation coefficients for the distribution of D between solvent and the initial states and, respectively, the transition states of all proton transfer reactions. This expression has been derived in the framework of semi-classical approximation as it supposes an equilibrium population of several transition states considered as some quasi-molecules. However, in reality, this equation is valid also for a pure quantum–mechanical mechanism of proton tunneling when the notion of some definite transition-state coordinates of proton loses its sense. The correct and general form of Eq. 20 is [45]

$$k_n = k_0 \overset{m}{\Pi}(1-n+n\gamma_i\phi_i)/\overset{m}{\Pi}(1-n+n\phi_i). \quad (20a)$$

Here, as before, ϕ_i are the fractionation coefficients for D distribution between solvent and reacting species (in the state *before* reaction), and γ_i are the ratios of true kinetic constants (D/H) at each reacting site. Eq. 20a transforms into Eq. 20 by substitution ϕ_i* for $\gamma_i\phi_i$: this substitution is strictly correct if transition state can be described semi-classically.

From Eq. 20a is seen that in the case of only one proton transferred and without isotopic enrichment of the reacting site ($\phi=1$) the k_n-n dependence is linear. At two or more protons involved the curve deviates from linearity. However, these deviations are not always well expressed. So, for two reacting protons with identical parameters the deviation at $n=0.5$ (close to the maximum one) equals to 11% for total $k_H/k_D=4$ ($\gamma=0.5$), 7% for $k_H/k_D=3$, and 3% for $k_H/k_D=2$. It is clear that the method can give reliable results only for substantial k.i.e.

4.7. Isotope effect on reorganization energy

In principle, isotopic substitution somewhat changes the dielectric properties of solvents, and hence should change the coupling constant C, and, correspondingly, reorganization energy (here $C=1/\varepsilon_o-1/\varepsilon_s$, ε_o and ε_s being optical and static dielectric constants). Using experimental data on ε_o and ε_s of heavy and light water, one can calculate that for D_2O reorganization energy should be higher only by 0.07%. However, it was shown by the spectral Stokes shift method [46] that water shows some anomalies in its behavior. Its reorganization energy is markedly higher than it could be expected in comparison with several aprotic solvents and even alcohols. This can be related to specific features of water as a liquid with a tridimensional network of hydrogen bonds. A substantial role of hydrogen bonds in the abnormal component of reorganization energy is confirmed by an isotope effect in reorganization energy about 2.5% [46]; this exceeds markedly the value calculated in the framework of continuum electrostatics. For enzymatic reactions, the difference between reorganization energies in H_2O and D_2O should be lower because only some part of reorganization energy (most probably, less than a half) is due to water reorganization.

4.8. Is a substantial primary k.i.e. inevitable in any rate-determining proton transfer reaction?

The answer to this question should be definitely *not*. As it is clear from the preceding discussion, *usually the main reason for k.i.e. is the difference in tunneling probabilities for the light and heavy isotopes, but not the difference in their zero-point energies.* The difference in zero energies is present always, and hence, in the framework of the bond-stretching model, should always result in a difference of activation energies, i.e. in a substantial k.i.e. (except imag-

inary, but highly improbable case of equal zero energies both in initial and transition states).

In contrast to that, the reorganization–tunneling model points clearly to the situation where the primary k.i.e. can be practically absent. When the tunneling probability for both (or even three) isotopes is high enough that the process becomes adiabatic (transmission coefficients in Eq. 4 equal to one), the difference between tunneling probabilities for these isotopes disappears. It was shown recently [47] that for a totally adiabatic process another reason for k.i.e. can exist. As was discussed in Section 3.2, at this regime a marked splitting of vibrational energy levels takes place, and this lowers activation energy by $E/2$ (more strictly, by $2\Delta E\alpha(1-\alpha)$, so the effect has its maximum at symmetric barrier, $\alpha = 1/2$). As the splitting for different isotopes is different, activation energies become different, and this causes a k.i.e. Adiabatic regime is possible under condition of fairly strong interaction of the initial and final states, in our case, of proton acceptor and donor. The extent of the splitting depends on the strength of their interaction. So, if the hydrogen bond is strong enough to make the process close to the totally adiabatic one, but not too strong to produce a large vibrational levels splitting, the k.i.e. becomes very small. With a further increase in the hydrogen bond strength, k.i.e. increases.

An important reservation should be made here. An intermediate case can exist when, at the same tunneling distance, proton transfer is adiabatic, but not that for deuteron. The latter can go over to an adiabatic regime at a shorter distance, but for this purpose some additional repulsion should be overcome, and D transfer will have somewhat higher activation energy than H transfer. So, under these conditions, some k.i.e. could be observed, but its magnitude would be lower than for the case of totally non-adiabatic transfers.

An additional contribution can be expected at $\Delta pK \neq 0$. As has been explained before (Section 4.4), at real ΔpK, there is a small difference in reaction energy and, hence, in activation energy. At $\Delta pK = \pm 6$ the corresponding rate constants ratios are of order of 1.1 and 0.9. The effect of involvement of excited vibrational states, based on the gain in tunneling probability, seems to be insubstantial for adiabatic transfer.

For a totally adiabatic process, some effect can originate also from different effective frequencies of classical subsystem, ω_{eff} (see Eq. 4). This frequency can be influenced by the isotopic substitution. For instance, when the reaction coordinate includes relative motion of two water molecules, the corresponding frequency can differ by $(20/18)^{1/2} = 1.05$ times (the ratio of masses of D_2O and H_2O).

Summing up, we can conclude that, at strong enough (but not too strong) interaction between proton donor and acceptor (good hydrogen bond), a regime close to the adiabatic one may appear, which results in low k.i.e.

One interesting case of a seemingly high k.i.e. for reactants forming a good hydrogen bond presents an acid-base reaction with diffusion limitations. When the rate of proton recombination with a base is determined by diffusional collision of reactants, the rate of the reverse reaction, the dissociation of the corresponding acid, is determined by diffusion of products from the cage where they were formed. Concentration of the products in the cage is determined by dissociation constant, and this is strongly affected by the difference of zero-point energies. So, the measured k.i.e. is, as a matter of fact, not a kinetic effect proper, but reflects the shift of the dissociation equilibrium.

5. Conclusions

The proton transfer presents one of the most frequent processes in chemical and biochemical reactions. A rigorous treatment of this phenomenon demands, first of all, for a consistent account of quantum–mechanical behavior typical of proton. Second, proton transfer is connected, in most cases, with charge transfer, and hence with a change of charge interaction with the medium polarization. The latter behaves classically.

On this physical basis, the following mechanism of proton transfer has been formulated and developed during the last three decades. As a result of classical thermal fluctuations of the medium polarization (and, if applicable, of other components of the classical subsystem), the energy levels of proton in its initial and final states become equal, and at that moment an underbarrier proton transition (tunneling)

becomes possible. The probability of the process is determined, first, by the probability to reach the top of the barrier along the classical coordinate(s), and, second, the probability of proton tunneling under isoenergetic conditions. Depending on the subsystems parameters, one can discern three main regimes. First is the totally adiabatic regime, when both electrons and proton follow adiabatically the classical subsystem movement, all of them remaining in the ground states; in this regime, the proton transfer probability at the top of the barrier equals to one. Second is the partially adiabatic regime, when electrons follow adiabatically the proton movement, but the latter does not follow classical subsystem. The tunneling probability at the top of the barrier is less than 1. The lowest transfer probability takes place at the totally non-adiabatic regime, where both proton and electrons undergo underbarrier transition with probabilities less than 1.

The property which is especially sensitive to quantum–mechanical nature of proton movement, is the kinetic isotope effect. In treatment of this phenomenon, it is often not sufficient to restrict oneself with simple models, but is necessary to account for subtle effects affecting markedly the experimental results. Among such effects, two of them deserve a special mention. First is the necessity for proton donor and acceptor to approach at the distance optimum for tunneling. This distance is usually different for different isotopes. The second effect is the possibility of involvement of the vibrationally excited states. The extent of this involvement is also different for different isotopes.

The reorganization–tunneling mechanism explains well, at least semi-quantitatively, the main experimental regularities of the proton transfer process. To the contrary, classical or semi-classical description of proton motion, being inconsistent from the theoretical point of view, cannot describe, even qualitatively, the total set of experimental data.

Acknowledgements

I thank Prof. A.M. Kuznetsov for critical reading of this paper and many useful observations. This work has been supported in part by grants from RFBR (99-04-48652) and INTAS (93-2852).

References

[1] J. Horiuti, M. Polanyi, Acta physicochim. URSS 2 (1935) 505–532.
[2] R.P. Bell, The Proton in Chemistry, Chapman and Hall, London, 1973.
[3] R.P. Bell, The Tunnel Effect in Chemistry, Chapman and Hall, London, 1980.
[4] L. Melander, W.H. Saunders, Jr., Reaction Rates of Isotopic Molecules, John Wiley and Sons, New York, 1980.
[5] R.R. Dogonadze, A.M. Kuznetsov, V.G. Levich, Elektrokhimiya (Russian) 3 (1967) 739–742.
[6] R.R. Dogonadze, A.M. Kuznetsov, V.G. Levich, Electrochim. Acta 13 (1968) 1025–1044.
[7] M.A. Vorotyntsev, R.R. Dogonadze, A.M. Kuznetsov, Dokl. Akad. Nauk SSSR (Russian) 209 (1973) 1135–1139.
[8] E.D. German, R.R. Dogonadze, A.M. Kuznetsov, J. Chem. Soc. Faraday Trans. II 76 (1980) 1128–1146.
[9] E.D. German, A.M. Kuznetsov, J. Chem. Soc. Faraday Trans. II 77 (1981) 2203–2212.
[10] L.I. Krishtalik, Charge Transfer Reactions in Electrochemical and Chemical Processes, Plenum, New York, 1986.
[11] L.I. Krishtalik, Faraday Discuss. Chem. Soc. 74 (1982) 205–213.
[12] D. Borgis, J.T. Hynes, J. Phys. Chem. 100 (1996) 1118–1128.
[13] A. Warshel, Z.T. Chu, J. Chem. Phys. 93 (1990) 4003–4026.
[14] R.I. Cukier, J. Phys. Chem. 100 (1996) 15428–15443.
[15] D. Antoniou, S.D. Schwartz, Proc. Natl. Acad. Sci. USA 94 (1997) 12360–12365.
[16] J. Ulstrup, Charge Transfer Processes in Condensed Media, Lecture Notes in Chemistry, Vol. 10, Springer-Verlag, Berlin, 1979.
[17] A.M. Kuznetsov, Charge Transfer in Physics, Chemistry and Biology. Physical Mechanisms of Elementary Processes and an Introduction to the Theory, Gordon and Breach, Reading, 1995.
[18] A.M. Kuznetsov, J. Ulstrup, Electron Transfer in Chemistry and Biology, John Wiley and Sons, Chichester, 1998.
[19] R.R. Dogonadze, A.M. Kuznetsov, Elektrokhimiya (Russian) 3 (1967) 1324–1330.
[20] E.A. Moelwyn-Hughes, Physical Chemistry, Pergamon Press, London, 1961.
[21] D.F. Calef, P.G. Wolynes, J. Phys. Chem. 87 (1983) 3387–3400.
[22] H. Sumi, R.A. Marcus, J. Chem. Phys. 84 (1986) 4894–4914.
[23] L.D. Zusman, Electrochim. Acta 36 (1991) 395–399.
[24] D. Xu, K. Schulten, Chem. Phys. 182 (1994) 91–117.
[25] A.V. Kotelnikov, V.R. Vogel, A.V. Pastuchov, V.L. Voskoboinikov, E.S. Medvedev, in Biological Electron Transfer Chains: Genetics, Composition and Mode of Operation, G.V. Canters, E. Vijgenboom (Eds.), Kluwer Academic Publishers, NATO ASI Series, Serie C: Mathematical and Physical Sciences, Vol. 512, 1998, pp. 29–51.
[26] L.I. Krishtalik, Kinetika i kataliz (Russian) 20, 847–853/J. Electroanalyt. Chem. 100 (1979) 547–561.
[27] H. Azzouz, D. Borgis, J. Chem. Phys. 98 (1993) 7361–7374.

[28] R. Pomès, B. Roux, Biophys. J. 71 (1996) 19–39.
[29] W.W. Cleland, M.H. O'Leary, D.B. Northrop (Eds.), Isotope Effects on Enzyme-Catalyzed Reactions, University Park Press, Baltimore, MD, 1977.
[30] R.D. Gandour, R.L. Schowen (Eds.), Transition States of Biochemical Processes, Plenum, New York, 1978.
[31] P.F. Cook (Ed.), Enzyme Mechanism from Isotope Effects, CRC Press, Boca Raton, FL, 1991.
[32] D.L. Purich (Ed.), Methods in Enzymology, Vol. 87, Enzymes Kinetics and Mechanism, Part C, Section IV, Academic Press, New York, 1992.
[33] D.L. Purich (Ed.), Methods in Enzymology, Vol. 249, Enzymes Kinetics and Mechanism, Part C, Section IV, Academic Press, New York, 1995.
[34] D.E. Khoshtariya, V.V. Topolev, L.I. Krishtalik, Bioorganicheskaya Khim. (Russian) 4 (1978) 1341–1351.
[35] D.E. Khoshtariya, V.V. Topolev, L.I. Krishtalik, I.L. Reizer, V.P. Torchilin, Bioorganicheskaya Khim. (Russian) 5 (1979) 1243–1247.
[36] D.E. Khoshtariya, Bioorganicheskaya Khim. (Russian) 4 (1978) 1341–1345.
[37] T. Jonsson, M.H. Glickman, S. Sun, J.P. Klinman, J. Am. Chem. Soc. 118 (1996) 10319–10320.
[38] B.J. Bahnson, J.P. Klinman, in: D.L. Purich (Ed.), Methods in Enzymology, Vol. 87, Enzymes Kinetics and Mechanism, Part C, Section IV, Academic Press, New York, 249 1995, pp. 373–397.
[39] A. Kohen, J.P. Klinman, Acc. Chem. Res. 31 (1998) 397–404.
[40] Y. Cha, C.J. Murray, J.P. Klinman, Science 243 (1989) 1325–1330.
[41] L.I. Krishtalik, Zh. Fiz. Khim. (Russian) 31 (1957) 2403–2413.
[42] L.I. Krishtalik, L.V. Bunakova, S.E. Shumskaya, Elektrokhimiya (Russian) 34 (1998) 1354–1360.
[43] D.M. Blow, Acc. Chem. Res. 9 (1976) 145–152.
[44] K.B. Schowen, R.L. Schowen, in: P.F. Cook (Ed.), Enzyme Mechanism from Isotope Effects, CRC Press, Boca Raton, FL, 1991, pp. 551–584.
[45] L.I. Krishtalik, Mendeleev Commun. 1993, pp. 66–67.
[46] L.I. Krishtalik, E.L. Mertz, V.V. Topolev, in: A.A. Kornyshev, M. Tosi, J. Ulstrup, (Eds.), Electron and Ion Transfer in Condensed Media, World Scientific, Singapore, 1997, pp. 372–401.
[47] A.M. Kuznetsov, Stochastic and Dynamic Views of Chemical Reaction Kinetics in Solutions, Press Polytechniques et Universitaires Romandes, Lausanne, 1999.